Key hydraulic drivers and patterns of fine sediment accumulation in gravel streambeds: a conceptual framework illustrated with a case study from the Kiewa River, Australia

Roser Casas-Mulet[1,2,§], Knut T. Alfredsen[3], Alexander H. McCluskey[2,4] and Michael J. Stewardson[2]

[1]Water Research Institute, Cardiff University, The Sir Martin Evans Building, Museum Avenue, Cardiff, CF10 3AX, UK

[2]Department of Infrastructure Engineering, The University of Melbourne, Melbourne, 3010, Australia

[3]Department of Hydraulic and Environmental Engineering, Norwegian University of Science and Technology, Trondheim, 7491, Norway

[4]Chair of Hydromechanics, Technical University of Munich, 80333, Munich, Germany

[§]corresponding author: casas-muletr@cardiff.ac.uk

Abstract

Fine sediment processes in gravel beds may have significant impacts to overall river ecosystem function. In addition to gravitational deposition, horizontal intragravel transport has been recognized to influence fine sediment accumulation. However, the specific hydraulic mechanisms and origin of fine sediment movement are not clearly identified. The purpose of this study was to investigate key hydraulic drivers and patterns of fine sediment accumulation. Using a conceptual framework to set the scene, we implemented an experimental setup in a gravel lateral bar subject to irregular flow fluctuations in the Kiewa River (Australia). We installed nine sets of sediment collector pairs and piezometers into the gravel. Each pair included one horizontally and one horizontally-vertically perforated collector. Mid-range, rather than peak flows, covering the site in water drove fine sediment deposited in the collectors. We estimated horizontal contribution to final deposition as 59%. Such contribution resulted from shear stresses >3 N m^{-2} promoting streamwise near-bed turbulence at the water-sediment interface during flooded conditions. Despite high subsurface hydraulic gradients, intragravel transport in the lower sediment layers via Darcy flow did not show any influence to fine

sediment deposition. Our findings contribute to an improved understanding of fine sediment accumulation processes, key for overall river ecosystem functioning, particularly in regulated rivers.

Running head: Hydraulic drivers and patterns of fine sediment accumulation

Keywords: fine sediment deposition and accumulation; hydraulic drivers; horizontal transport; upper and lower sediment layers

Highlights

- A conceptual model of the key hydraulic drivers of fines accumulation is presented.
- A case study in the Kiewa River (Australia) is used to assess the model parameters.
- Horizontal sources contributed 59% to final deposition.
- Near-bed transport in the upper sediment layers was identified as the main mechanism for deposition.

- Intragravel transport in the lower sediment layers was not a significant driver.

Graphical Abstract

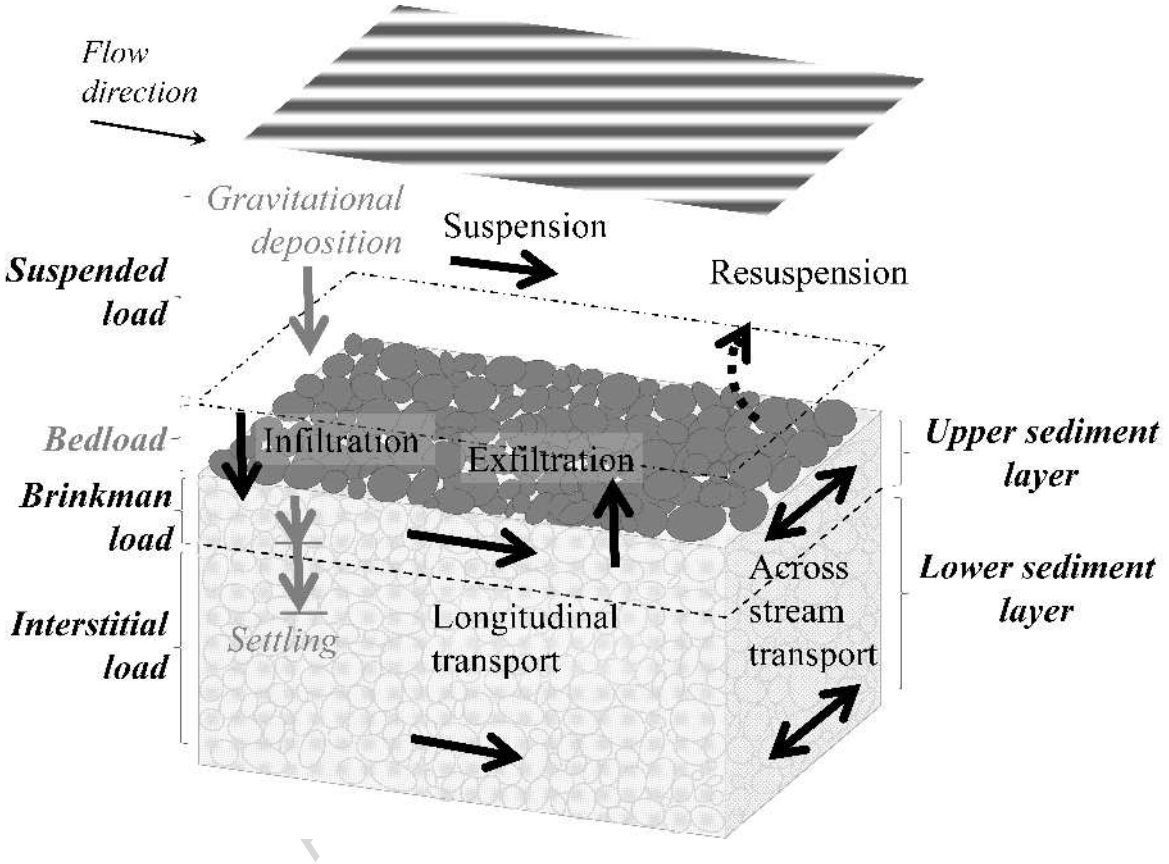

1. Introduction

Fine sediments (< 2 mm) can be deposited and accumulated within gravel and cobble streambeds via infiltration of sand and smaller sediments (Carling, 1984; Zimmermann and Lapointe, 2005). Transport and retention of fines into riverbeds is a natural process facilitating matrix development (Frostick et al., 1984; Lisle, 1989; Sear, 1993). However, anthropogenic activities - such as river regulation and land clearance - affect fluxes of fine suspended sediment in fluvial systems and increase local sediment deposition within gravel streambeds (Owens et al., 2005; Denic and Geist, 2015). This can result in adverse environmental impacts (Sear, 1993; Franssen et al., 2014) including: changed sub-surface flow patterns (Petticrew et al., 2007); reduced permeability and intragravel flow (Brunke, 1999; Simpson and Meixner, 2012; Stewardson et al., 2016); decreased oxygen availability (Soulsby et al., 2001); inhibited water, pollutant and nutrient exchange across the sediment-water interface (Findlay et al., 1993); and potentially degraded habitats and aquatic organisms (Greig et al., 2005; Jones et al., 2012; Buendia et al., 2013; Mathers and Wood, 2016). Understanding the mechanisms leading to fine sediment accumulation along and across streambeds is therefore key for comprehending human impacts on river ecosystems.

Models of fine sediment transport into gravels usually assume a non-slip condition at the sediment-water interface and consider gravitational settling alone (Biedenharn et al., 2008). Consequently, gravitational deposition from the *suspended load* (Fig. 1) is the most widely attributed mechanism to accumulation of fine sediment in the streambed (Einstein, 1968; Beschta and Jackson, 1979; Frostick et al., 1984; Lisle, 1989; Schälchli, 1992; Gibson et al., 2009; Hamm et al., 2011; Boano et al., 2014; Evans and Wilcox, 2014; Huston and Fox, 2015). However, suspended sediment may be advected into the porous matrix (Lisle, 1989; Schälchli, 1992; Brunke, 1999). Downwelling and upwelling of water

associated with pressure gradients at the sediment-water interface (Elliott and Brooks, 1997; Mathers and Wood, 2016) may produce both infiltration and exfiltration of suspended sediment by advective transport (Savant et al., 1987; Tonina and Buffington, 2009). Such pressure gradients are induced by geomorphological features including bedforms (Elliott and Brooks, 1997; Packman et al., 2004), local heterogeneity, roughness and permeability in the streambed (Boulton et al., 1998; Cardenas et al., 2004). Infiltration may then lead to settling within the pore spaces deeper in the streambed (Stewardson et al., 2016), or promote further transport of the fine sediment along or across the sediment matrix (Fig. 1). Fines may be deposited in the streambed or re-suspended in the water column via exfiltration from the sediment column (Schindler Wildhaber et al., 2012; Eder et al., 2014; Schindler Wildhaber et al., 2014) (Fig. 1).

In addition, turbulence generated by large-scale flow structures and smaller scale local obstructions on the bed may promote shear instability in the boundary layer above the sediment-water interface. It may generate turbulent mixing into the upper layers of the sediment bed (Brayshaw et al., 1983; White and Nepf, 2007; Manes et al., 2009; Boano et al., 2011; Grant et al., 2012), to depths up to 2-10 times the mean diameters of the bed material (Tonina and Buffington, 2009). The upper sediment layer influenced by the water column is known as the Brinkman layer (Boudreau, 1997; Boudreau and Jorgensen, 2001), in which the velocity of fluid particles decreases with depth until it reaches an averaged constant velocity that is predicted by the Darcy equation. In this study, we refer to *Brinkman load* as the area in the upper sediment layers where transport occurs due to the influence of the water column (Fig. 1).

Below the Brinkman layer, Darcian flow driven by hydraulic gradients (Fetter, 2001; Hassan et al., 2015) may produce transport through the interstitial spaces of the sediment matrix. We refer to the transport in these lower sediment layers as *Interstitial load* (Fig. 1). Such horizontal transport is almost certainly very small relative to total stream load and may only occur if pore velocities exceed the threshold for initiation of motion (Franssen et al., 2014).

Horizontal intragravel transport of fine sediments has been considered in several recent studies (Sear, 1993; Soulsby et al., 2001; Greig et al., 2005; Petticrew et al., 2007; Sear et al., 2008; Franssen et al., 2014; Mathers and Wood, 2016), but few have attempted to quantify its relative contribution to total deposition. Sear (1993) attributed 20-25% of infiltrated sediments to intragravel motion through the gravels. Carling (1984) and Seydell et al. (2009) found ~ 30% difference in trapping efficiency from permeable to impermeable walled pots in flumes. In contrast, Petticrew et al. (2007) found 24% less fine sediments in permeable walled compared to impermeable walled collectors, attributing sediment loss owing to vertical resuspension during controlled reservoir releases. Finally, Franssen et al. (2014) made indirect estimations, concluding that intragravel flows could not transport fine sediment. Although comparisons between studies are difficult to generalize because of different measurement methodologies and use of terms (Sear et al., 2008; Schindler Wildhaber et al., 2012), such differing results highlight that our knowledge of the relative contribution of horizontal mechanisms and hydraulic-related drivers of fine sediment deposition is limited. Moreover, there is no comprehensive clear framework defining the origin and the hydraulic mechanisms driving fine sediment accumulation (e.g., upper or lower sediment layers and surface or subsurface mechanisms dominance).

Considering fine sediments as those that accumulate within the coarse gravel matrix and may include sand-sized sediments, we used a literature-based conceptual model (Fig. 1) and a case study in the regulated Kiewa River (SE Australia) to address three specific questions:

(i) What are the overall patterns of fine sediment accumulation?

(ii) What are the key hydraulic drivers influencing fine sediment deposition?

(iii) What is the relative contribution of horizontal *vs.* vertical sources to fine sediment accumulation?

2. Methods

2.1. Study site

The Kiewa River is a regulated tributary of the Murray River (North Victoria, Australia, Fig. 2) with a total catchment area of 1750 km^2, 109 km in length, and elevation range between 156 and 681 m.a.s.l.. Lower temperatures and higher precipitation promote some snow between April and October at the southern end of the basin (Newall et al., 2006). The regulated Kiewa River system includes the Rocky Valley Reservoir (Fig. 2), which releases water for hydroelectric power generation at several stations. Changes of flow caused by such storage releases can be large and rapid, with several fluctuations each day. The West Kiewa Power station discharges to a regulating pondage at Mount Beauty (Fig. 2) that serves to smooth out the fluctuations in the flow before the water is released back into the West Kiewa River (Lawrence, 2001). We implemented a

field program in a 50 m x 30 m homogenous lateral gravel bar located 600 m below the regulating pondage in the West Kiewa River, in a 0.004 sloped reach (Fig. 2). The natural Kiewa sediment consists of a non-homogenous matrix ranging from coarse to very coarse gravel. Approximately 40-45% of sediments are smaller than 9.5 mm and 20% of sediments are smaller than 2 mm, with grains between 0.85 and 0.35 mm dominating the lower fractions of bed material (see section 2.2 for additional details).

Upstream *vs.* site hydrographs (Fig. 3) illustrate that hydropower releases from the pondage in the West Kiewa River occurred only during the early part of the study period, from mid-February until mid-March. Maximum water levels at the study site during these conditions were below 346.1 m.a.s.l. (approximately 10.6 m^3 s^{-1}), leaving the drawdown zone (area subject to fluctuating water levels) almost entirely dewatered at the gravel surface. After mid-March, as a result of major refurbishment works at the West Kiewa Power Station (Fig. 2), regulated flows were replaced by a natural regime. These higher base flows promoted flooded conditions (water levels at or above the gravel surface) in parts of the study site. However, only three major natural flood events (>346.3 m.a.s.l., >16.42 m^3 s^{-1}) in March, April and June 2013, covered the entire drawdown zone in water. High amounts of total suspended solids (TSS) were delivered during these peak events, when discharges reached 19.5 m^3 s^{-1} and water levels reached 346.4 m.a.s.l. (Fig. 3).

2.2. Data collection

Twenty-four sediment collectors were initially installed at the site to assess rates of fine sediment deposition. The collectors' design was based on the one presented in Lachance and Dubé (2004), specially purposed to use in gravel beds for avoiding loss of fines during collection and retrieval. Each collector was composed of two impermeable walled cylinders (dimensions: 0.11 m radius, 0.2 m height) positioned one inside the other. Several 9.5 mm holes were perforated in each cylinder. The holes of the inside and outside cylinders were aligned, so a small turn in the inside container could open or close the holes (Fig. 4). The perforated walls allowed horizontal infiltration in all 24 collectors. Half of the collectors had closed lids and were impermeable in the bottom to prevent vertical sediment influx filling in the pore space (H collectors). The other 12 collectors were perforated in the bottom and had perforated lids to allow vertical sediment infiltration (HV collectors). Before field installation, each collector was pre-filled with non-homogenous graded sediment obtained from the Kiewa riverbed and truncated at the >9.5 mm fraction. We used the natural bed granulometry curves as a reference to calculate the percentage of coarser fractions needed to pre-fill each initial collector. We constructed the curves from three sediment samples previously obtained from the study site. They were each approximately 0.2 m in depth and 0.008 m^3 in volume. Each sample was dried (100°C for 24 h) and passed through a set of standard nested sieves (128, 90, 60, 45, 32, 22.5, 16, 9.5, 4.75, 2.36, 0.85, 0.35 mm). The resulting range of granulometry curves provided information on the relative weight of the coarser fractions (Fig. 5), so we distributed the truncated material as evenly as possibly across all collectors before field installation.

Nine pairs of collectors (one each of H and HV) were inserted into the gravel bed, each inside a 0.008 m^3 hole with the collector's top at the surface gravel level (Fig. 4). We filled the small gap between the sediment matrix and the collector's wall with coarse (>9.5 mm) sediment fractions to avoid immediate contact with unstable fines falling into the collectors by artificially created mechanisms.

A set of six collectors (two pairs of H and HV) was distributed along each of three transects within the drawdown zone (Fig. 2). As references, two additional collector pairs (W1 and W3) were placed in the permanently wet area, and one pair (D) in the permanently dry bank (Fig. 2). Collectors were installed on 24 January and their positions were recorded using a Leica Geosystems® Viva (Switzerland) differential Global Positioning System. Nine 0.032 m inside diameter and 0.5-0.7 m length Durapipe® (UK) piezometers were installed into the river bed (at ca. 0.4 m depth) next to each collector pair (Fig. 2). Each piezometer contained an Eijkelkamp® (The Netherlands) Diver water pressure transducer providing continuous 5-min resolution data of surface or subsurface water levels (±0.005 m accuracy). The perforated holes in each collector were closed during installation and opened *in situ* immediately afterwards to allow sediment collection (Fig. 4).

Each set of collector pairs (H and HV at A, B, C locations) were retrieved and re-installed every 4-8 weeks from one of the upstream, middle or downstream transects (Fig. 2). Each collector was closed immediately before retrieval to avoid fine sediment loss (Fig. 4). A new pre-filled collector was installed immediately at the same location after each retrieval. All collectors were finally retrieved from the site on 2 July. Thirty out of the thirty-eight samples were retrieved successfully (Table 1) and were taken to the lab for particle size distribution analysis. Eight

collectors were lost owing to unknown reasons (potentially vandalism given the proximity to a camping site). Five sets of data corresponding to five different periods were obtained (Table 1).

2.3. Data analysis

2.3.1. Sediment accumulation patterns

After field retrieval, sediment samples from the collectors were first dried (100°C for 24 h) and put through a set of standard nested fine sieves (2.36, 0.85, 0.35 mm), with 2.36 mm being the coarser size of the sediments infiltrated and deposited into the collectors. Each fraction was then recovered and weighed and used to construct granulometry curves. Organic matter ratios (%) were estimated for each collector using the combustion method of Bretschko and Leichtfried (1987), and deducted from the total fine sediment fraction.

The total accumulation in each of the collectors was computed for each fine sediment fraction and for the total fines. Accumulation rates were expressed in kg d^{-1} to allow comparable units between H and HV collectors. Rates in the drawdown area were compared with the rates in the wet and dry reference areas for each collector type and sampling period. Location-averaged accumulation rates provided information on trends of deposition along and across the gravel.

We carried out a non-parametric Wilcoxon Signed Rank test to assess differences between individual H and HV collector pairs in the drawdown area (n=30). The relative contribution of horizontal and vertical sediment sources was then calculated for individual collector pairs. By deducting the proportional mass of accumulated sediment between H and HV individual collector pairs, the proportion of vertical and horizontal accumulation was obtained for each location and period.

In addition, to provide a context for comparison, we converted the accumulation rates in this study to kg m^{-2} d^{-1} (dividing it by the correspondent H and HV collectors' area). We then selected several similar field studies in the literature for which their accumulation rates were expressed or could be converted to the same units, and hence compared to our study.

2.3.2. Antecedent sediment conditions

Grain and pore size distributions in the matrix may have a strong influence on fine sediment infiltration and accumulation (Frostick et al., 1984; Brunke, 1999). Mean grain size (represented by the diameter of the 50^{th} percentile (D_{50}) of a sample) and sediment sorting coefficients (S_o) were calculated for each individual collector before and after installation to assess the influence of antecedent sediment conditions to fine sediment accumulation. The sorting coefficient (S_o) can be expressed as:

$$So = \left(\frac{D_{75}}{D_{25}}\right)^{0.5} \quad (1)$$

where D_{75} and D_{25} represent the diameter of the 75th and 25th percentiles of the sample, respectively (Lotspeich and Everest, 1981; Petticrew et al., 2007).

2.3.3. Key hydraulic-related parameters

A total of eight hydraulic-related variables and variations in their values (maximum, minimum, cumulative sum, range, 25th percentile, 75th percentile) were the chosen parameters to represent the various transport mechanisms, load and media described in our conceptual model (Fig. 1). They could be estimated from field data and included surface and subsurface water levels, total suspended solids (TSS), bed shear stress, vertical hydraulic gradients and Darcy velocity. The list of parameters and variables are presented in Table 2 and the justification for their choice is explained below.

Maximum surface water levels and high suspended sediments are expected to promote high fine sediment accumulation through gravitational deposition (Acornley and Sear, 1999; Soulsby et al., 2001; Greig et al., 2005; Zimmermann and Lapointe, 2005), and could also potentially

encourage resuspension (Schindler Wildhaber et al., 2014). Continuous water levels and TSS data were therefore used to compute the magnitude, duration and range values during flooded conditions to assess such potential influence (Table 2).

Along and across riverbed subsurface transport or infiltration may be controlled by surface hydraulics, forcing fine sediments deeper into the bed or potentially flushing them from the surface gravel layers (Sear, 1993; Boano et al., 2011; Grant et al., 2012). These processes may be associated with turbulent mass and momentum transfer that will be dependent on shear stresses near the streambed (Schälchli, 1992). In order to assess such links, we calculated cross-sectionally averaged, steady, uniform channel bed shear stress (τ_b) as a representative parameter promoting infiltration into the bed or near-bed transport (*Brinkman load*, Table 2):

$$\tau_b = \rho g h S \quad (2)$$

where τ_b (N m^{-2}) is bed shear stress, ρ (kg m^{-3}) is the density of water, g (m s^{-2}) is the acceleration due to gravity, h (m) is the water depth, and S (m m^{-1}) is the slope of the riverbed (Leopold et al., 1964).

Transport in the Brinkman layer may also be driven by hyporheic upwelling and downwelling caused by localized pressure gradients forcing the water to flow across the streambed (Savant et al., 1987). We calculated vertical hydraulic gradients (VHG) as a common parameter to assess the upwelling and downwelling potential (Baxter et al., 2003). VHG were computed for each pair of collectors (from piezometers data) during

flooded conditions (Table 2). We used the difference in hydraulic head divided by the vertical distance between W and A/B/C piezometers (as in Hucks Sawyer et al., 2009; Casas‐Mulet et al., 2015).

Following Franssen et al. (2014), we used the Darcy velocity to determine the advective rate of horizontal flowing water through the pore spaces in the *Interstitial load* transport zone. We calculated Darcy velocity during both flooded and dewatered conditions (Table 2) as:

$$V = \frac{K\,dh}{n\,dl} \quad (3)$$

where V is Darcy velocity in the pore spaces (m s^{-1}), n is the effective substrate porosity, K (m s^{-1}) is the hydraulic conductivity and dh/dl (hydraulic gradient) is the hydraulic head divided by the horizontal distance between two piezometers (Fetter, 2001). Porosity and hydraulic conductivity were estimated from the grain size distribution of three 0.008 m^3 river bed samples. Porosity (n) was estimated using the method of Frings et al. (2008), which is an empirical predictor based on the entire grain size distribution of a sample. Hydraulic conductivity (K) was also derived from the grain size distribution using the Hazen method:

$$K = 100\,(D_{10})^2 \quad (4)$$

where D_{10} represents the diameter of the 10th percentiles of the sample and 100 is the constant used (in Franssen et al., 2014) for gravel beds. Hydraulic gradients were calculated in the lateral direction (using the A and C piezometers) for each of the continuous water level (surface and subsurface) measurements.

2.3.4. Drivers of fine sediment accumulation

Both antecedent sediment conditions (2.3.2) and hydraulic-related parameters calculated above were compared with fine sediment accumulation rates (kg d^{-1}) for each individual collector using regression to assess their role in driving accumulation. Resulting R^2 values were used to determine the strength of the relationship, considering R^2 = 0.7 to be the lower threshold of a strong relationship. A relationship was considered significant when $p < 0.05$.

2.3.5. Entrainment functions

To determine whether entrainment occurs in the Brinkman or upper sediment layers, we calculated critical shear stress (τ_c) for the finer sediment factions in the Kiewa River, represented by the diameter of the 10th percentiles of the sample (D_{10}). We then compared τ_c to bed shear stress (τ_b)

calculated in Eq. (2). Critical shear stress was found by undertaking dimensionless analysis $\tau_c^* = f(D^*)$ with the modified Shields diagram (Shields, 1936; Vanoni, 1975), where τ_c^* is the dimensionless critical shear stress and D^* the dimensionless diameter:

$$\tau_c^* = \frac{\tau_c}{D(\rho_s - \rho_w)g} \quad (5a)$$

$$D^* = \frac{D}{v}\sqrt{gD\frac{\rho_s - \rho_w}{\rho_w}} \quad (5b)$$

where ρ_s is the density of sediment material (kg m^{-3}) and v is the kinematic viscosity of water (m^2 s^{-1}).

Shear stress is assumed to be greatest at the sediment-water interface and to decline with an exponential decay of the velocity with depth in the Brinkman layer (Nagaoka and Ohgaki, 1990). We compared Darcy velocities to shear velocities as an indication of the significance of transport in the lower sediment layers (*Interstitial load*). Shear velocities u_* (m s^{-1}) at the sediment-water interface were calculated as:

$$u_* = \sqrt{\frac{\tau_b}{\rho_w}} \quad (6)$$

This comparison only provided a qualitative assessment, as we did not calculate subsurface sediment transport rates, nor take into account stresses produced by inter-porous flows.

3. Results

3.1. Patterns of fine sediment accumulation

Fine sediment accumulated in the drawdown area weighed 1.2±0.8 (*av.*±*std*) kg, and accumulations rates were 0.01 kg d^{-1} on average, ranging between 0.0005 and 0.06 kg d^{-1} (Table 3). There was no significant (p=0.1) difference in accumulation rates between the drawdown and the permanently wet areas in the Kiewa River. But they were significantly (p<0.05) higher (10.2 times) in the drawdown area than in the dry zones.

Longitudinally, the middle transect (A2-C2) showed higher accumulation rates in both H and HV collectors, tied to the accumulation that occurred during periods P2 and P5. Secondary lateral patterns of fine sediment accumulation were also observed in both collector types, with higher accumulation rates closer to the thalweg (Fig. 6).

By periods, the lowest fine sediment accumulations occurred during P1, with similar rates to those in the dry areas. The highest rates were found in period P5, considerably higher than the other periods P2, P3 and P4, which presented mid-range accumulation rates (Fig. 7). The proportion of sediment fractions remained similar for all periods, with dominance of the middle (<0.8 mm) fractions (Fig. 7).

Outcomes of the Wilcoxon Signed-Rank Test showed that H collectors elicited a statistically significant decrease in fine sediment accumulation compared to HV collectors (Z= –2.81, p=0.005). Fine sediment in HV collectors was higher in 10 out of 13 samples (Table 4). The negative ranks and ties illustrated in Table 4 refer to the sediment accumulated during period P1, when only dewatered conditions prevailed. For periods P2 to P5, therefore, differences in accumulation rates were 41% higher (in mean) in HV compared to H collectors (Table 5), inferring that the relative rate of horizontal infiltration during flooded or semi-flooded conditions in the gravel was a mean of 59% (Table 5).

3.2. Drivers of fine sediment accumulation

3.2.1. Antecedent sediment conditions

Values of D_{50} and S_o in the pre-filled collectors before field installation (Table 3) did not show significant relationships to accumulation rates according to Pearson correlation tests (p=0.143 for D_{50} and p=0.88 for S_o). As expected, retrieved sediment samples with trapped fines showed a decrease in D_{50} (2% in P1, and 63% in P5), and an increase in S_o (between 6%, in period P1 and 389%, in P5). The content of organic matter in the collected samples ranged from 2-16% (Table 3) and it was not correlated to sediment accumulation rates (p=0.48).

3.2.2. Flooded vs. dewatered conditions in the gravel

On average, water levels were below the top of the collectors 93.3% of the time (Fig. 7), as a result of dominantly dewatered conditions in the gravel. As expected, collectors A (located closer to the thalweg, Fig. 2) were exposed to flooded conditions for longer durations than collectors C (located closer to the bank). By periods, collectors in P5 were exposed to flooded conditions the longest (water levels >346.1 m.a.s.l.), whilst collectors in P1 were mostly exposed to dewatered conditions, with water levels ≤346.1 m.a.s.l. (Fig. 8).

Hydraulic gradients were very steep in the lateral direction during dewatered conditions, particularly in the middle transect (up to 0.04 m m^{-1}). Subsurface water tended to flow towards the bank and no signs of return flow from the bank to the thalweg were found. During flooded conditions, hydraulic gradients were milder and oriented downstream along the channel (Fig. 9).

3.2.3. Key hydraulic-related parameters

Strong and significant correlations were found between fine sediment accumulation rates and surface water levels, TSS and bed shear stress during flooded conditions (Table 6). However, accumulation rates did not show any significant or strong relationship with any of the tested parameters during dewatered conditions.

The strongest and most significant correlations are illustrated in Fig. 10. TSS values varied between 12.6 mg L^{-1} (in the first period, P1), and 72.1 mg L^{-1} in P5. Mean bed shear stress values ranged from 0 to 4.1 N m^{-2}, with highest values found in P4 and P5. Given low accumulation rates in P1, the graph (Fig. 10, left) suggests that little sediment is accumulated during periods when bed shear stress is less than 1.5 N m^{-2}.

Mean VHG ranged between -0.25 and 0.08 m m^{-1} with a dominance of negative values. VHGs generally decreased with distance to the thalweg (Table 7), but they did not show any relationship with fines accumulation (Table 6). Darcy velocities varied between 0 and 0.004 m s^{-1} with average values of 0.0015 m s^{-1}. During dewatered conditions, because of steeper hydraulic gradients (Fig. 9), Darcy velocities reached higher values (0.001 m s^{-1}) than during flooded conditions. However, no relationships were found with fine sediment accumulation (Table 6).

Entrainment functions demonstrated that mean shear stress values (τ_b) exceeded critical stress ($\tau_c = 0.31\ N\ \ m^{-2}$) for the smallest sediment fractions (D_{10}) in all locations for all periods (Table 7), suggesting shear velocities were more than sufficient to transport fine sediments within the upper sediment-water interface layers *(Brinkman load)*. However, Darcy velocities were several orders of magnitude less than the calculated shear velocities at the sediment-water interface (Table 7) in all locations, periods and conditions (flooded and dewatered). These indicate no motion and supported the above results in suggesting Darcy fluxes are unlikely to promote sediment transport in the lower sediment layers *(Interstitial load).*

4. Discussion

Patterns of sediment accumulation indicate the importance of sediment processes operating at the bar-scale. Higher accumulation in the middle transect may indicate local differences in sediment coarseness and roughness (Sear, 1993; Acornley and Sear, 1999; Schindler Wildhaber et al., 2012) rather than a strong longitudinal pattern. Secondary lateral patterns with higher accumulation rates closer to the thalweg could be explained by longer durations of water covering such locations and promoting fine sediment exchange. These link to periods of longer exposure to flooded or semi-flooded conditions having higher accumulation rates than periods of dominantly dewatered conditions (e.g., P1).

When compared with other studies on fine sediment accumulation in the literature, the overall rates in the Kiewa River fall into the lower range of accumulation rates (Table 8) both regarding vertical and horizontal infiltration. Despite low accumulation rates in the study site, presumably caused by dominantly dewatered conditions, our estimate of 59% contribution from horizontal sources is rather high. This is particularly the case compared to other examples in the literature (~ 20-30% in Carling, 1984; Sear, 1993; Seydell et al., 2009). However, site-specific differences between studies suggest comparisons of fine sediment accumulation need to be made with care (Schindler Wildhaber et al., 2012; Franssen et al., 2014).

Dewatered conditions indeed dominated in the site during the experiments and subsurface flows were the only possible transport mechanisms during P1, as surface water levels did cover the collectors. In such conditions, both the upper and lower sediment layers *(Brinkman* and

Interstitial load) would most likely have a similar behavior given there was no influence of surface hydraulics. Therefore, the very small accumulation of fines during the first period (~ 0.01 kg d^{-1}) could have only occurred horizontally through the sediment layer. However, no relationship was found between Darcy flow and fine sediment accumulation, and Darcy fluxes were significantly lower than the threshold of motion in all cases. These could suggest that interstitial movement has no effect on sediment accumulation, or that any potential influence of horizontal processes in the lower sediment layers could not be captured through our setup or estimation approach. Experiments with an adequate setup for such observations should be used for this purpose (see Casas-Mulet et al., submitted).

Flooded conditions resulted from a combination of natural peak flows and mid-range flows covering the study site (water levels >346.1 m.a.s.l.). They drove most of the fine sediment accumulation in both H and HV collectors. Given the strong relationship found between fine sediment accumulation rates and TSS, it could be assumed that the majority of fine sediment accumulation in the collectors was driven by gravitational deposition derived from one of the three peak events in March, April and June, providing high amounts of sediment in suspension. However, the dominant fractions accumulated in the collectors were mid-sized (around 0.8 mm) in all samples, indicating that the infiltrated sediment originated from a fine fraction of bedload rather than much finer settled suspended load (Lisle, 1989; Petticrew et al., 2007; Schindler Wildhaber et al., 2014). In addition, the strong relationship between fine sediment and τ_b suggests that the infiltration occurred when τ_b> 3 N m^{-2}. Then, surface hydraulics induced mixing (Packman et al., 2004; Tonina and Buffington, 2009) into the *Brinkman load* zone and the finer fractions of the Kiewa River could be entrained in the bed.

Since the strongest correlations were found with mean rather than maximum shear stress, we deduced that reaching and maintaining mid-range flows (water levels >346.1 m.a.s.l.) was a stronger driver of infiltration than reaching the peak maximum (346.4 m.a.s.l.). This assumption is supported by the high accumulation rates found in periods P2 and P5, in which bed shear stress did not reach the highest values. However, changes in supply during the study period should also be considered to explain such variations.

Resuspension was not considered to have any influence on fine sediment accumulation given the consistent higher amounts of fine sediment in HV collectors compared to H indicating vertical loss of sediments was unlikely. Exfiltration and infiltration mechanisms promoted through vertical upwelling and downwelling were considered to play a limited role in fine sediment accumulation in the Kiewa River, as no significant relationships were found between accumulation rates and VHG values.

Despite its broad use, we recognize limitations in the field method applied for fine sediment collection as artificial conditions could be promoted in the collectors. The limitation of the method is most relevant during the studied dewatered conditions, where intragravel movement in the lower sediment layers was potentially the only source of infiltration. Given the scale and scope of the present work, we were unable to directly observe the specific relative contribution of *Interstitial vs. Brinkman load* to horizontal fine sediment accumulation. Very low accumulation rates during P1 suggest interstitial transport could be considered negligible but could not be directly quantified here. Interstitial transport may play a key role in redistributing fine sediment in gravel beds (Petticrew et al., 2007) and its estimation may be relevant in high gradient streams; in areas with sudden changes in sediment porosity; in reaches subject to extreme floods; and/or in newly restored reaches where new clean gravel

may be filled in with fines. Such estimation should be investigated further with studies at the adequate spatial and temporal scales and currently remains and interesting area for further research.

5. Conclusions

Based on a conceptual model illustrated with a case study in the Kiewa River (Australia), we provide a framework to distinguish key hydraulics drivers of fine sediment accumulation during dewatered and flooded conditions in gravel beds. With local hydraulics driving patterns of accumulation, most deposition occurred during flooded conditions was caused by near-bed turbulence occurring in the top sediment-water interface. Contrary to what we expected, peak flows promoting high suspension of fines did not drive accumulation. Instead, shear velocities occurring during long-lasting mid-range flows were highly correlated with accumulated fines. Horizontal sources of fine sediment accounted for more than half of the accumulation in the collectors, suggesting the dominance of lateral/streamwise transport during flooded conditions. The few fines that accumulated in the collectors during dewatered conditions were presumably transported through interstitial processes in the lower sediment layers. However, because these could not be quantified or analytically verified via entrainment functions, this remains a gap in knowledge. Overall, our work provides a framework to distinguish between the origin (upper *vs*. lower sediment layers) and direction (horizontal

vs. vertical) of fine sediment accumulation in gravel beds. It also highlights the importance of fully understanding such driving mechanisms to inform river management practices, key for overall river ecosystem functioning, particularly in regulated rivers.

Acknowledgements

This work was carried out as part of the Australian Government Endeavour Research Fellowship awarded to Casas-Mulet. Work was also supported by the Australian Research Council through two projects DP130103619 and LP130100174. The authors would like to thank the adjacent to the site land owners and North East Catchment Management Authority (NECMA) to help grant access to the site, and AGL for the provision of data. Thanks to Prof. Stanley Grant and Dr Markus Noack for feedback on a very early draft and to Dr. Gregory Pasternack for providing very useful comments at the final stages. Last, but not least, our most sincere thanks Rodger Young and Judit Castillo for the invaluable help in the field.

References

Acornley, R.M., Sear, D.A., 1999. Sediment transport and siltation of brown trout (Salmo trutta L.) spawning gravels in chalk streams. Hydrological Processes, 13(3), 447-458.

Baxter, C., Hauer, F.R., Woessner, W.W., 2003. Measuring groundwater–stream water exchange: new techniques for installing minipiezometers and estimating hydraulic conductivity. Transactions of the American Fisheries Society, 132(3), 493-502.

Beschta, R.L., Jackson, W.L., 1979. The intrusion of fine sediments into a stable gravel bed. Journal of the Fisheries Board of Canada, 36(2), 204-210.

Biedenharn, D., Watson, C., Thorne, C., 2008. Fundamentals of fluvial geomorphology. ASCE, Sedimentation Engineering; Processes, Measurements, Modeling and Practice, 355-386.

Boano, F., Harvey, J.W., Marion, A., Packman, A.I., Revelli, R., Ridolfi, L., Wörman, A., 2014. Hyporheic flow and transport processes: Mechanisms, models, and biogeochemical implications. Reviews of Geophysics, 52(4), 603-679.

Boano, F., Revelli, R., Ridolfi, L., 2011. Water and solute exchange through flat streambeds induced by large turbulent eddies. Journal of Hydrology, 402(3-4), 290-296.

Boudreau, B.P., 1997. Boundary conditions, Diagenetic models and their implementation. Modelling transport and reactions in aquatic sediments. Springer.

Boudreau, B.P., Jorgensen, B.B., 2001. The benthic boundary layer: Transport processes and biogeochemistry. Oxford University Press, Oxford.

Boulton, A.J., Findlay, S., Marmonier, P., Stanley, E.H., Valett, H.M., 1998. The functional significance of the hyporheic zone in streams and rivers. Annual Review of Ecology and Systematics, 59-81.

Brayshaw, A.C., Frostick, L.E., Reid, I., 1983. The hydrodynamics of particle clusters and sediment entrapment in coarse alluvial channels. Sedimentology, 30(1), 137-143.

Bretschko, G., Leichtfried, M., 1987. The determination of organic matter in river sediments. Veröffentlichungen der Arbeitsgemeinschaft Donauforschung, 403-417.

Brunke, M., 1999. Colmation and depth filtration within streambeds: retention of particles in hyporheic interstices. International Review of Hydrobiology, 84(2), 99-117.

Buendia, C., Gibbins, C.N., Vericat, D., Batalla, R.J., Douglas, A., 2013. Detecting the structural and functional impacts of fine sediment on stream invertebrates. Ecological indicators, 25, 184-196.

Cardenas, M.B., Wilson, J., Zlotnik, V.A., 2004. Impact of heterogeneity, bed forms, and stream curvature on subchannel hyporheic exchange. Water Resources Research, 40(8).

Carling, P.A., 1984. Deposition of fine and coarse sand in an open-work gravel bed. Canadian journal of fisheries and Aquatic Sciences, 41(2), 263-270.

Casas-Mulet, R., Lakhanpal, G., Stewardson, M.J., submitted. The relative contribution of near-bed vs. intragravel horizontal movement to fine sediment processes in river gravel beds. Geomorphology.

Casas-Mulet, R., Alfredsen, K., Hamududu, B., Timalsina, N.P., 2015. The effects of hydropeaking on hyporheic interactions based on field experiments. Hydrological Processes, 29(6), 1370-1384.

Denic, M., Geist, J., 2015. Linking stream sediment deposition and aquatic habitat quality in pearl mussel streams: implications for conservation. River Research and Applications, 31(8), 943-952.

Eder, A., Exner-Kittridge, M., Strauss, P., Blöschl, G., 2014. Re-suspension of bed sediment in a small stream–results from two flushing experiments. Hydrology and Earth System Sciences, 18(3), 1043-1052.

Einstein, H.A., 1968. Deposition of suspended particles in a gravel bed. Journal of the Hydraulics Division, 94(5), 1197-1206.

Elliott, A.H., Brooks, N.H., 1997. Transfer of nonsorbing solutes to a streambed with bed forms: Theory. Water Resources Research, 33(1), 123-136.

Evans, E., Wilcox, A.C., 2014. Fine sediment infiltration dynamics in a gravel-bed river following a sediment pulse. River Research and Applications, 30(3), 372-384.

Fetter, C.W., 2001. Applied hydrogeology. Prentice hall.

Findlay, S., Strayer, D., Goumbala, C., Gould, K., 1993. Metabolism of streamwater dissolved organic carbon in the shallow hyporheic zone. Limnology and Oceanography, 38(7), 1493-1499.

Franssen, J., Lapointe, M., Magnan, P., 2014. Geomorphic controls on fine sediment reinfiltration into salmonid spawning gravels and the implications for spawning habitat rehabilitation. Geomorphology, 211(0), 11-21.

Frings, R.M., Kleinhans, M.G., Vollmer, S., 2008. Discriminating between pore-filling load and bed-structure load: a new porosity-based method, exemplified for the river Rhine. Sedimentology, 55(6), 1571-1593.

Frostick, L.E., Lucas, P.M., Reid, I., 1984. The infiltration of fine matrices into coarse-grained alluvial sediments and its implications for stratigraphical interpretation. Journal of the Geological Society, 141(6), 955-965.

Gibson, S., Abraham, D., Heath, R., Schoellhamer, D., 2009. Vertical gradational variability of fines deposited in a gravel framework. SEDIMENTOLOGY, 56(3), 661-676.

Grant, S.B., Stewardson, M.J., Marusic, I., 2012. Effective diffusivity and mass flux across the sediment-water interface in streams. Water Resources Research, 48(5).

Greig, S.M., Sear, D.A., Carling, P.A., 2005. The impact of fine sediment accumulation on the survival of incubating salmon progeny: Implications for sediment management. Science of The Total Environment, 344(1–3), 241-258.

Hamm, N.T., Dade, W.B., Renshaw, C.E., 2011. Fine particle deposition to porous beds. Water Resources Research, 47(11).

Hassan, M.A., Tonina, D., Beckie, R.D., Kinnear, M., 2015. The effects of discharge and slope on hyporheic flow in step-pool morphologies. Hydrological Processes, 29(3), 419.

Hucks Sawyer, A., Bayani Cardenas, M., Bomar, A., Mackey, M., 2009. Impact of dam operations on hyporheic exchange in the riparian zone of a regulated river. Hydrological Processes, 23(15), 2129-2137.

Huston, D.L., Fox, J.F., 2015. Clogging of fine sediment within gravel substrates: Dimensional analysis and macroanalysis of experiments in hydraulic flumes. Journal of Hydraulic Engineering, 141(8), 04015015.

Jones, J., Murphy, J., Collins, A., Sear, D., Naden, P., Armitage, P., 2012. The impact of fine sediment on Macro-Invertebrates. River Research and Applications, 28(8), 1055-1071.

Lachance, S., Dubé, M., 2004. A new tool for measuring sediment accumulation with minimal loss of fines. North American Journal of Fisheries Management, 24(1), 303-310.

Lawrence, R., 2001. The impacts of hydro-electric construction works on the hydrology of a subalpine area in Australia. Environmental Geology, 40(4-5), 612-621.

Leopold, L., Wolman, M., Miller, J., 1964. Fluvial Processes in Geomorphology Dover Publications Inc. New York, USA.

Lisle, T.E., 1989. Sediment transport and resulting deposition in spawning gravels, north coastal California. Water Resources Research, 25(6), 1303-1319.

Lotspeich, F.B., Everest, F.H., 1981. A new method for reporting and interpreting textural composition of spawning gravel, 369. US Dept. of Agriculture, Forest Service, Pacific Northwest Forest and Range Experiment Station.

Manes, C., Pokrajac, D., McEwan, I., Nikora, V., 2009. Turbulence structure of open channel flows over permeable and impermeable beds: A comparative study. Physics of Fluids (1994-present), 21(12), 125109.

Mathers, K.L., Wood, P.J., 2016. Fine sediment deposition and interstitial flow effects on macroinvertebrate community composition within riffle heads and tails. Hydrobiologia, 1-14.

Nagaoka, H., Ohgaki, S., 1990. Mass transfer mechanism in a porous riverbed. Water Research, 24(4), 417-425.

Newall, P., Bate, N., Metzeling, L., 2006. A comparison of diatom and macroinvertebrate classification of sites in the Kiewa River system, Australia. Hydrobiologia, 572(1), 131-149.

Owens, P., Batalla, R., Collins, A., Gomez, B., Hicks, D., Horowitz, A., Kondolf, G., Marden, M., Page, M., Peacock, D., 2005. Fine-grained sediment in river systems: environmental significance and management issues. River Research and Applications, 21(7), 693-717.

Packman, A.I., Salehin, M., Zaramella, M., 2004. Hyporheic exchange with gravel beds: basic hydrodynamic interactions and bedform-induced advective flows. Journal of Hydraulic Engineering, 130(7), 647-656.

Petticrew, E.L., Krein, A., Walling, D.E., 2007. Evaluating fine sediment mobilization and storage in a gravel-bed river using controlled reservoir releases. Hydrological Processes, 21(2), 198-210.

Savant, S.A., Reible, D.D., Thibodeaux, L.J., 1987. Convective transport within stable river sediments. Water Resources Research, 23(9), 1763-1768.

Schälchli, U., 1992. The clogging of coarse gravel river beds by fine sediment. Hydrobiologia, 235-236(1), 189-197.

Schindler Wildhaber, Y., Michel, C., Burkhardt-Holm, P., Bänninger, D., Alewell, C., 2012. Measurement of spatial and temporal fine sediment dynamics in a small river. Hydrology and Earth System Sciences, 16(5), 1501-1515.

Schindler Wildhaber, Y., Michel, C., Epting, J., Wildhaber, R., Huber, E., Huggenberger, P., Burkhardt-Holm, P., Alewell, C., 2014. Effects of river morphology, hydraulic gradients, and sediment deposition on water exchange and oxygen dynamics in salmonid redds. Science of the Total Environment, 470, 488-500.

Sear, D.A., 1993. Fine sediment infiltration into gravel spawning beds within a regulated river experiencing floods: Ecological implications for salmonids. Regulated Rivers: Research & Management, 8(4), 373-390.

Sear, D.A., Frostick, L.B., Rollinson, G., Lisle, T.E., 2008. The significance and mechanics of fine-sediment infiltration and accumulation in gravel spawning beds. In: D.A. Sear, D. P. (Eds.), Salmonid Spawning Habitat in Rivers: Physical Controls, Biological Responses, and Approaches to Remediation. Symposium, 65, Bethesda, USA, American Fisheries Society, pp. 149-174.

Seydell, I., Ibisch, R.B., Zanke, U.C., 2009. Intrusion of suspended sediments into gravel riverbeds: influence of bed topography studied by means of field and laboratory experiments. Advances in Limnology, 61, 67-85.

Shields, A., 1936. Application of similarity principles and turbulence research to bed-load movement, Soil Conservation Service, Pasadena, California.

Simpson, S.C., Meixner, T., 2012. Modeling effects of floods on streambed hydraulic conductivity and groundwater-surface water interactions. Water resources research, 48(2), W02515.

Soulsby, C., Youngson, A.F., Moir, H.J., Malcolm, I.A., 2001. Fine sediment influence on salmonid spawning habitat in a lowland agricultural stream: a preliminary assessment. Science of The Total Environment, 265(1–3), 295-307.

Stewardson, M., Datry, T., Lamouroux, N., Pella, H., Thommeret, N., Valette, L., Grant, S., 2016. Variation in reach-scale hydraulic conductivity of streambeds. Geomorphology, 259, 70-80.

Tonina, D., Buffington, J.M., 2009. Hyporheic exchange in mountain rivers I: Mechanics and environmental effects. Geography Compass, 3(3), 1063-1086.

Vanoni, V., 1975. Sediment discharge formulas. Sedimentation Engineering, edited by VA Vanoni, 190-229.

White, B.L., Nepf, H.M., 2007. Shear instability and coherent structures in shallow flow adjacent to a porous layer. Journal of Fluid Mechanics, 593, 1-32.

Zimmermann, A., Lapointe, M., 2005. Intergranular flow velocity through salmonid redds: sensitivity to fines infiltration from low intensity sediment transport events. River Research and Applications, 21(8), 865-881.

Figures

Figure 1. Conceptual model of fine sediment transport (black arrows) and deposition (grey arrows) processes in gravel beds including three load regions (*Suspended load, Brinkman load* and *Interstitial load*) within the water and sediment columns in which such processes occur (left). The model proposes distinct modes of sediment transport in these three regions identified by transitions in the velocity profile V(y) (right).

Figure 2. Location of the West Kiewa River and the site (right map, modified from Lawrence, 2001) and location of collectors and piezometers within the study site (left).

Figure 3. Unregulated water levels 5 km upstream from the West Kiewa Power Station (upper graph, source: Department of Environment Water Land and Planning) and; regulated water levels and total suspended solids (TSS) at the study site 2 km downstream from the regulating pondage (bottom graph, TSS data source: AGL Hydro). Note: see Fig. 2 (left) for geographical location.

Figure 4. Pre-filling, installation, retrieval and sample extraction for the analysis of fine sediment accumulation in the collectors Note: Depicted for H collectors only.

Figure 5. Areas illustrating the range of grain size distribution curves for the natural river bed (n=3) and all pre-filled collectors (n=30) truncated at 9.5 mm before installation. Single lines depict the average grain size distribution of the final H (n=13) and HV (n=13) collectors.

Figure 6. Spatial distribution of fine sediment accumulation rates in the field site (Note that the upstream and middle transects are averages of two periods (P1 and P4 and P2 and P5, respectively), whilst the downstream transect is one period (P3).

Figure 7. Fine sediment accumulation rates for each period and location in the Kiewa River for H and HV collectors (top), and cumulative percentage of sediment fractions in each case (bottom).

Figure 8. Water levels relative to the collectors for each period and site. Dark grey indicates water levels above the top of the collector (surface water level) and light grey levels inside the collector (between the bottom and the top). Note: Illustration for HV collectors only.

Figure 9. Subsurface hydraulic gradients during dewatered and flooded hydraulic conditions in the study site.

Figure 10. Correlations between accumulated fine sediment rates at each location and mean bed shear stress (τ_b) and 75% of total suspended solids (TSS) for each relevant period. Note: the shaded areas in the left graph illustrated collectors grouped into periods.

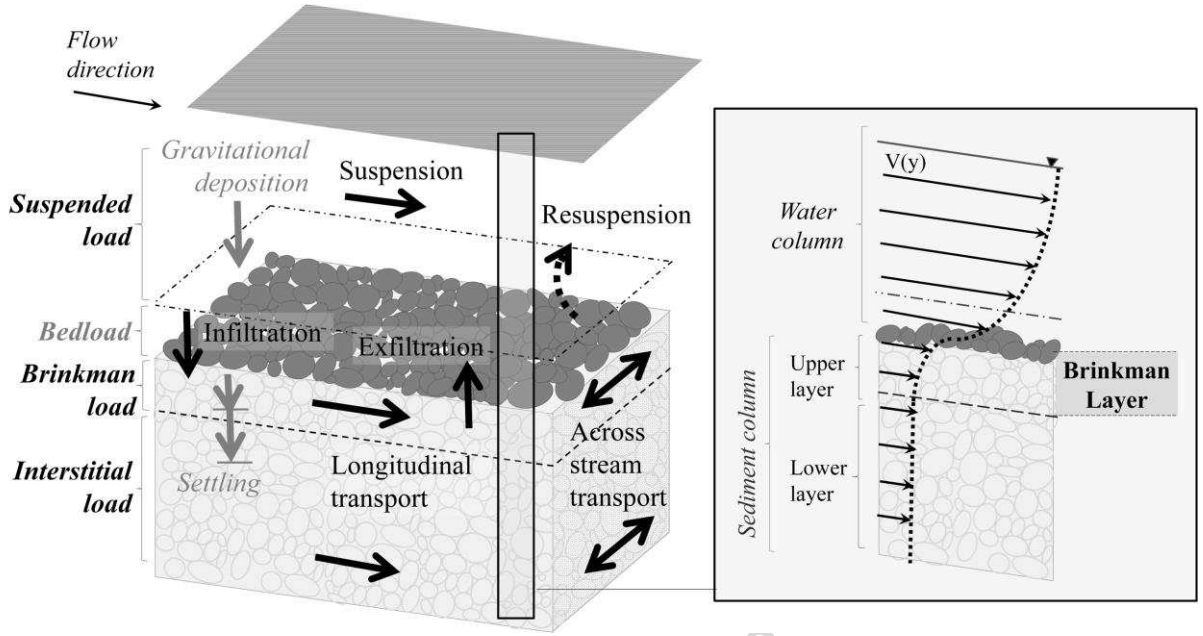

Figure 1

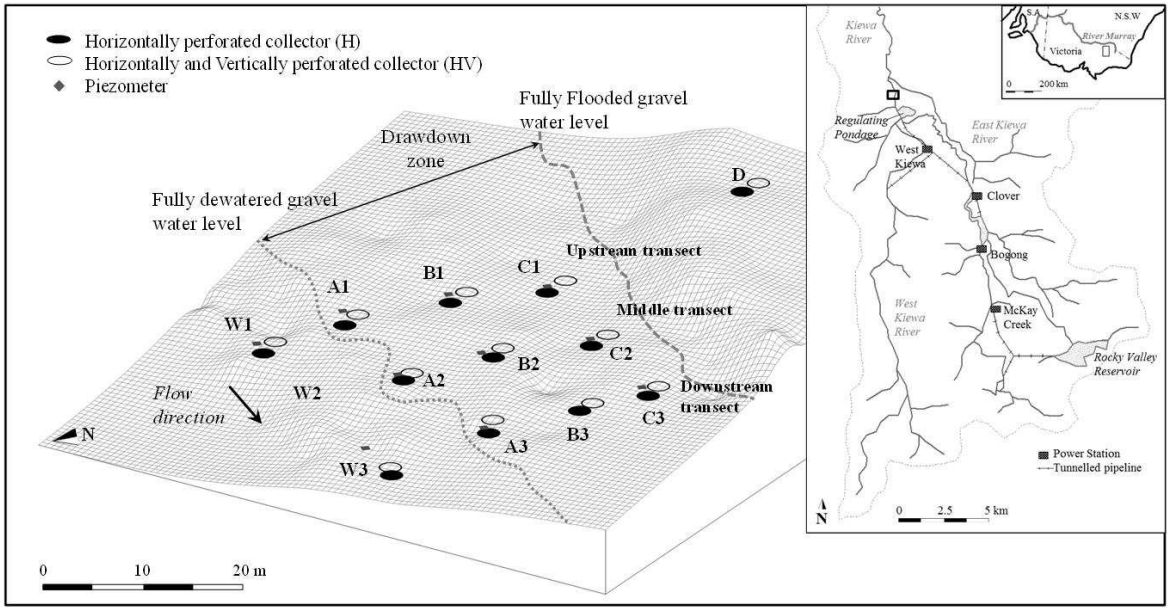

Figure 2

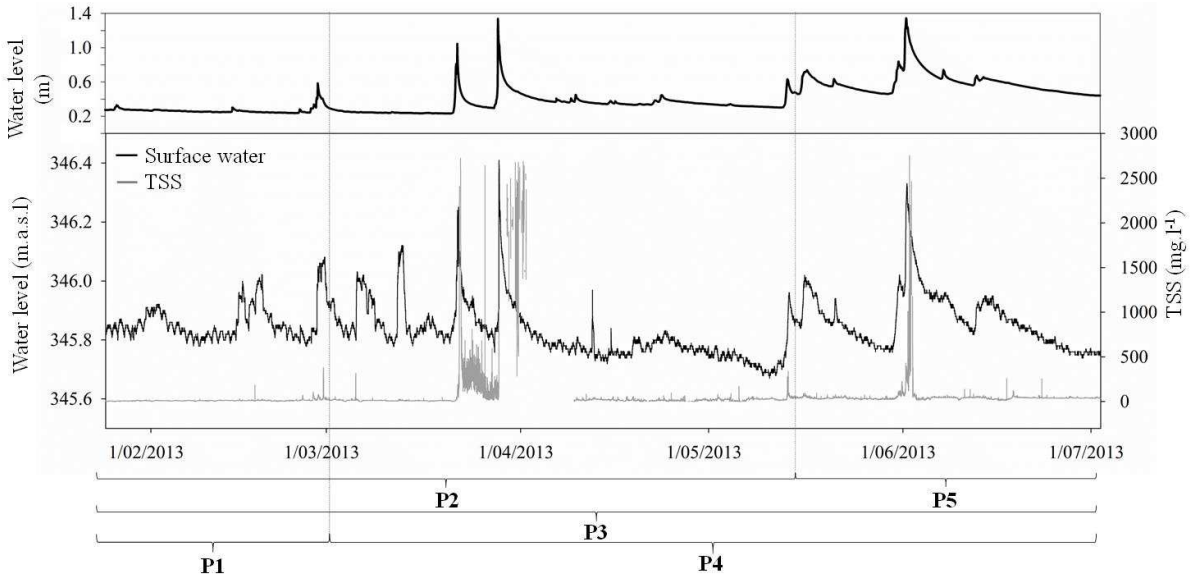

Figure 3

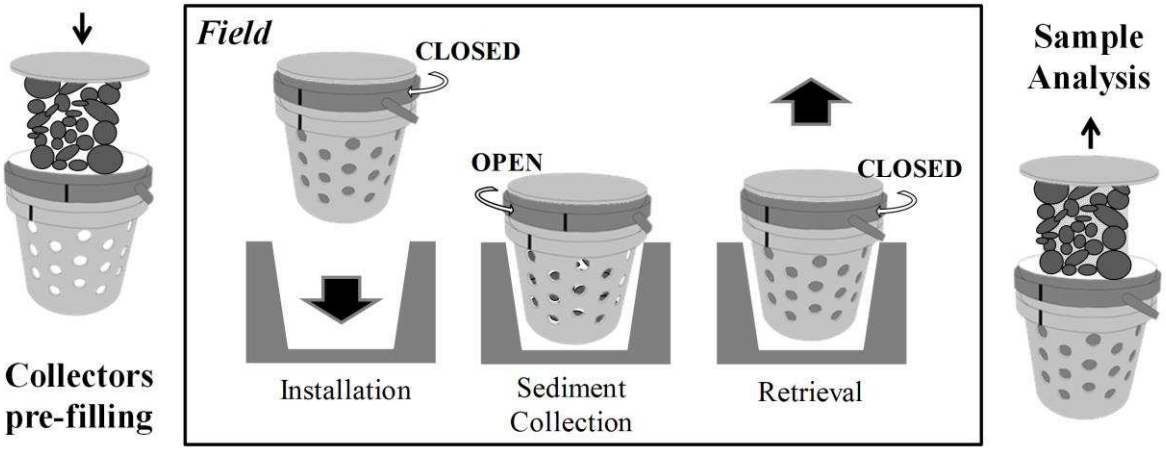

Figure 4

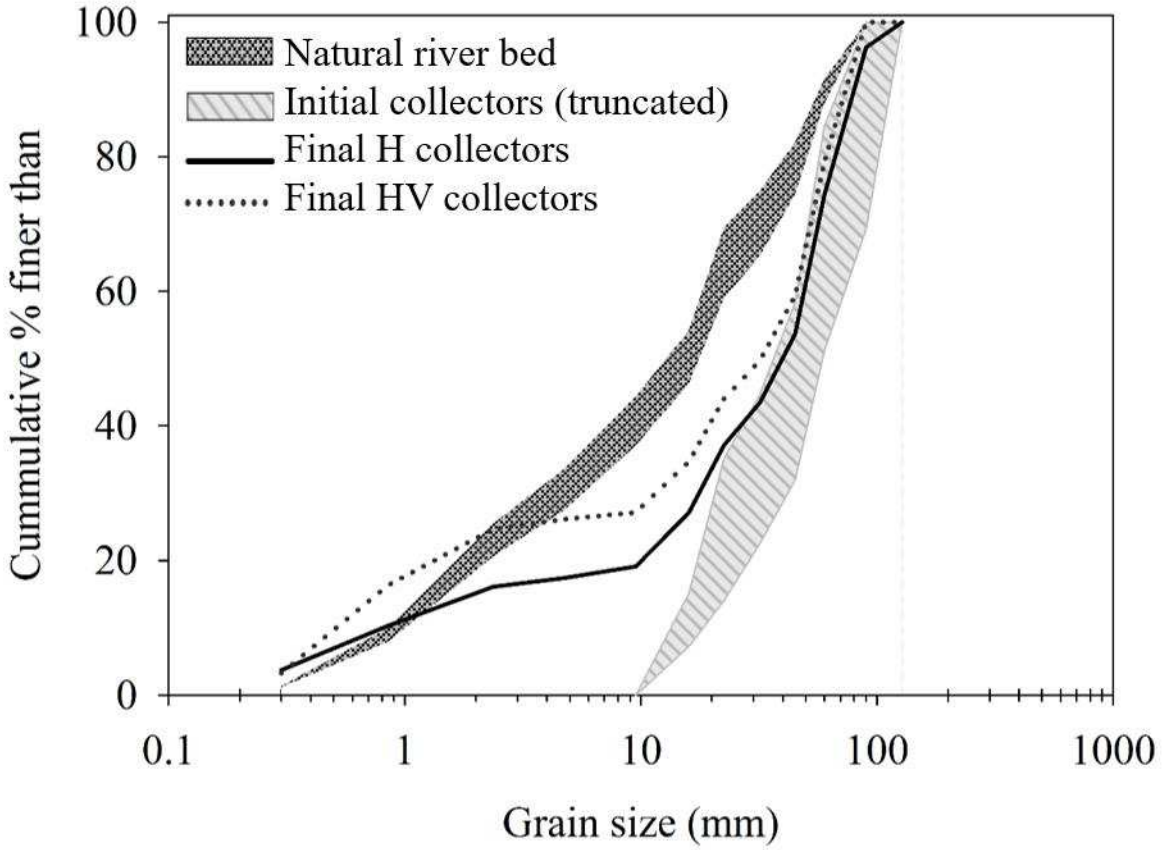

Figure 5

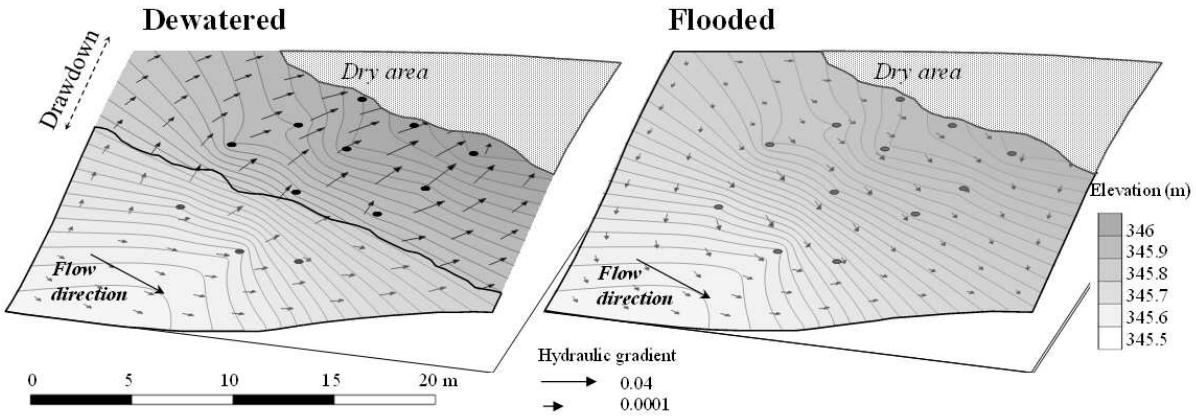

Figure 6

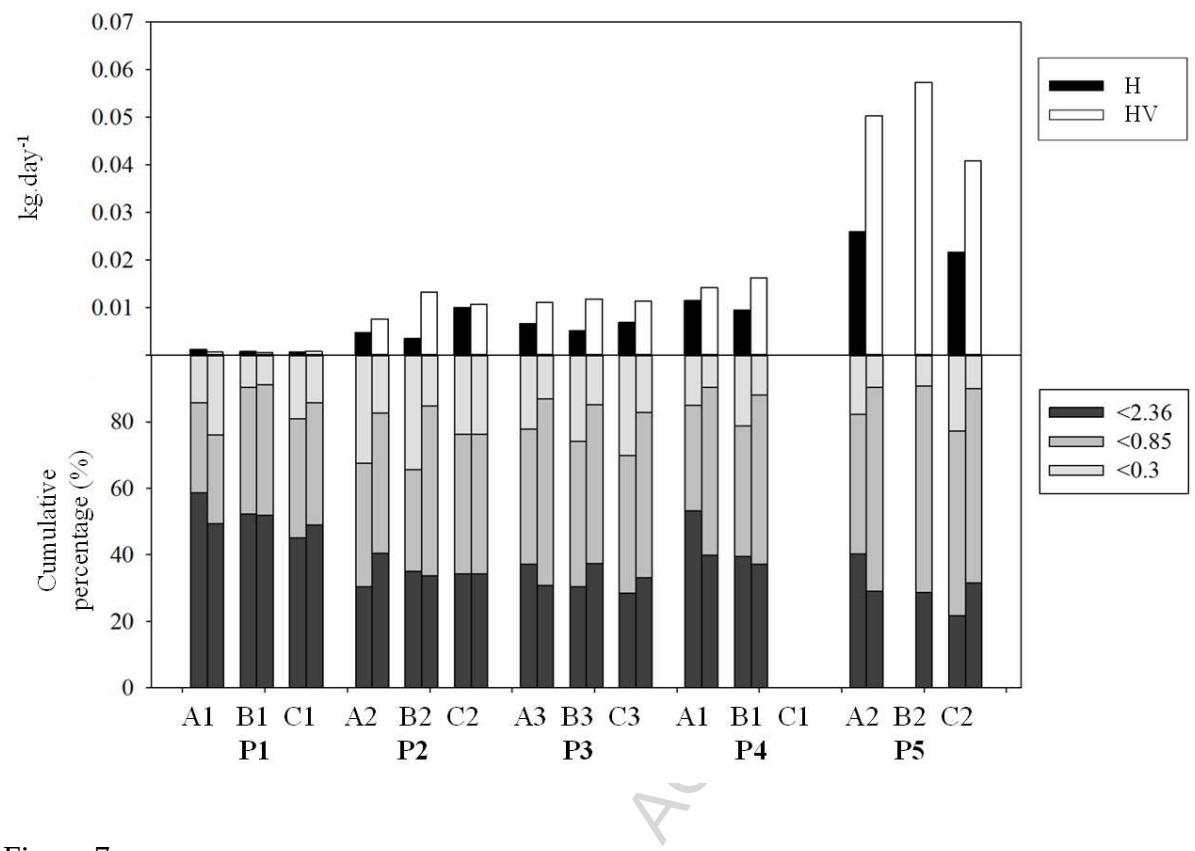

Figure 7

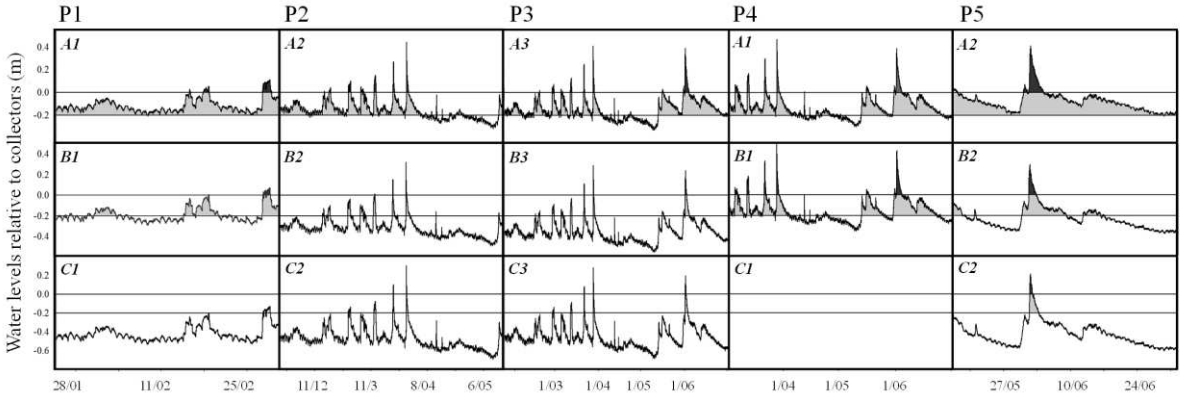

Figure 8

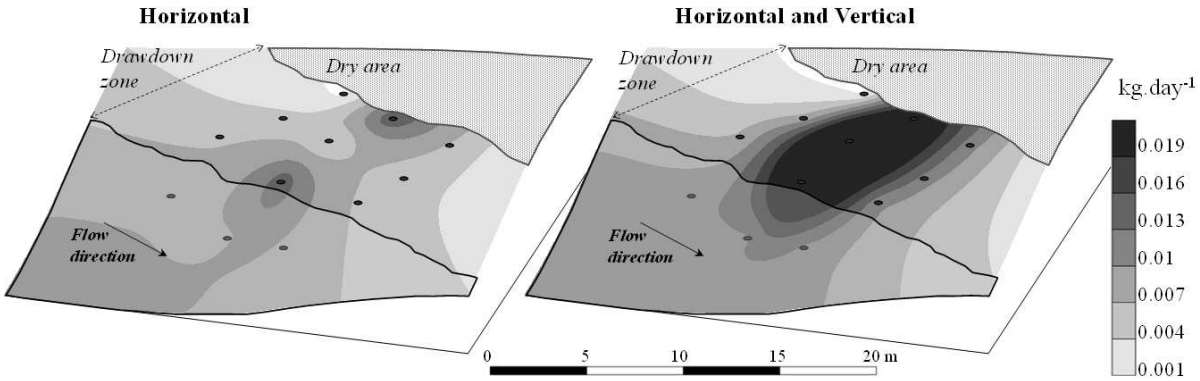

Figure 9

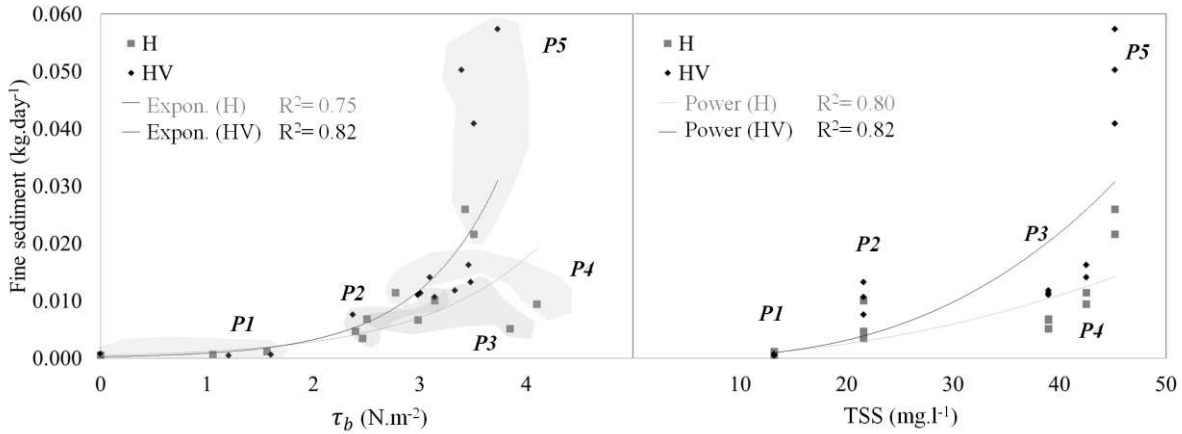

Figure 10